0026-895X/06/6906-1820–1828$20.00
MOLECULAR PHARMACOLOGY
Copyright © 2006 The American Society for Pharmacology and Experimental Therapeutics
Mol Pharmacol 69:1820–1828, 2006

Vol. 69, No. 6
20941/3115777
Printed in U.S.A.

Suppression and Regression of Choroidal Neovascularization by Systemic Administration of an $\alpha_5\beta_1$ Integrin Antagonist

Naoyasu Umeda, Shu Kachi, Hideo Akiyama, Grit Zahn, Doerte Vossmeyer, Roland Stragies, and Peter A. Campochiaro

Departments of Ophthalmology and Neuroscience, The Johns Hopkins University School of Medicine, Baltimore, Maryland (N.U., H.A., P.A.C.); and Jerini Pharmaceuticals, Berlin, Germany (G.Z., D.V., R.S.)

Received November 18, 2005; accepted March 9, 2006

ABSTRACT

Integrin $\alpha_5\beta_1$ plays an important role in developmental angiogenesis, but its role in various types of pathologic neovascularization has not been completely defined. In this study, we found strong up-regulation of $\alpha_5\beta_1$ in choroidal neovascularization. Implantation of an osmotic pump delivering 1.5 or 10 μg/h (~1.8 or 12 mg/kg/day) of 3-(2-{1-alkyl-5-[(pyridin-2-ylamino)-methyl]-pyrrolidin-3-yloxy}-acetylamino)-2-(alkylamino)-propionic acid (JSM6427), a selective $\alpha_5\beta_1$ antagonist, caused significant suppression of choroidal neovascularization; the area of neovascularization was reduced by 33 to 40%. When an osmotic pump delivering 10 μg/h of JSM6427 was implanted 7 days after rupture of Bruch's membrane, there was terminal deoxynucleotidyl transferase dUTP nick-end labeling (TUNEL) staining in vascular cells within the neovascularization and significant regression of the neovascularization over the next week. JSM6427 also induced apoptosis of cultured vascular endothelial cells. Fibronectin stimulates phosphorylation of extracellular signal-regulated kinase (ERK) in $\alpha_5\beta_1$-expressing cells that is blocked by JSM6427. These data suggest that $\alpha_5\beta_1$ plays a role in the development and maintenance of choroidal neovascularization and provides a target for therapeutic intervention.

Vascular endothelial cells participating in angiogenesis get signals from several sources. Surrounding tissue that senses the need for increased blood (oxygen) delivery is an important source of soluble stimulators. In hypoxic tissue, the transcription factor hypoxia inducible factor-1 (HIF-1) is stabilized, resulting in up-regulation of several genes (Manalo et al., 2005). Vascular endothelial growth factor (VEGF) is an important hypoxia-regulated soluble signal produced by surrounding tissue that promotes neovascularization. Things other than hypoxia, such as cytokines, also up-regulate VEGF, and in many instances, this seems to be through HIF-1 or HIF-2 (Bardos et al., 2004; Haddad and Harb, 2005). Although other soluble signals undoubtedly play a role, it is clear that inhibition of VEGF is a useful strategy for treatment of neovascular diseases (Ribatti, 2005).

This work was supported by the Foundation Fighting Blindness, the Macula Vision Foundation, and National Eye Institute grant EY12609. P.A.C. is the George S. and Dolores Dore Eccles Professor of Ophthalmology.

Article, publication date, and citation information can be found at http://molpharm.aspetjournals.org.

doi:10.1124/mol.105.020941.

Another source of signals is the extracellular matrix (ECM). The ECM seems capable of providing both stabilizing signals that suppress neovascularization and stimulatory signals (Sottile, 2004). Integrins are cell surface receptors that mediate signaling from the ECM, and signaling from ECM is modulated by alterations in the integrin population on the cell surface. Therefore, it is important to determine in any given situation which integrins mediate stimulation of neovascularization and which seem to suppress it.

Integrins $\alpha_v\beta_3$ and $\alpha_v\beta_5$ are up-regulated on endothelial cells participating in several types of neovascularization, including tumor vessels and retinal neovascularization (Brooks et al., 1994a,b; Luna et al., 1996). Antagonists of $\alpha_v\beta_3$ and $\alpha_v\beta_5$ suppress tumor neovascularization and retinal neovascularization (Hammes et al., 1996; Luna et al., 1996). However, the same antagonists of $\alpha_v\beta_3$ and $\alpha_v\beta_5$ that suppress retinal neovascularization, have no identifiable suppressive effect on choroidal neovascularization in mice (P. A. Campochiaro, unpublished data). Gene knockout studies have shown that deletion of α_v, β_3, and/or β_5 fails to block developmental angiogenesis and in some cases may enhance an-

ABBREVIATIONS: HIF-1, hypoxia inducible factor-1; VEGF, vascular endothelial growth factor; ECM, extracellular matrix; FGF2, fibroblast growth factor 2; PBS, phosphate-buffered saline; TBS, Tris-buffered saline; ERK, extracellular signal regulated kinase; ONL, outer nuclear layer; BSA, bovine serum albumin; PI, propidium iodide; GSA, *Griffonia simplicifolia* lectin; TUNEL, terminal deoxynucleotidyl transferase dUTP nick-end labeling; DAPI, 4,6-diamidino-2-phenylindole; HRP, horseradish peroxidase; BSA, bovine serum albumin; JSM6427, 3-(2-{1-alkyl-5-[(pyridin-2-ylamino)-methyl]-pyrrolidin-3-yloxy}-acetylamino)-2-(alkylamino)-propionic acid.

giogenesis (Hynes, 2002). Therefore, it seems that the role of integrins in neovascularization in one situation does not guarantee participation in a different vascular bed and different disease process.

Integrin $\alpha_5\beta_1$ is also up-regulated on activated endothelial cells and tumor blood vessels (Collo and Pepper, 1999; Kim et al., 2000; Magnussen et al., 2005; Parsons-Wingerter et al., 2005). Antagonists of $\alpha_5\beta_1$ suppress angiogenesis on chick chorioallantoic membrane induced by FGF2, tumor necrosis factor-α or interleukin-8 and in murine tumor models (Kim et al., 2000; Stoeltzing et al., 2003; Magnussen et al., 2005). Integrin $\alpha_5\beta_1$ also plays a critical role in developmental angiogenesis (Yang et al., 1993; Hynes, 2002). During vascularization of the central nervous system, angiogenic sprouts express high levels of $\alpha_5\beta_1$, and it is markedly reduced as the vessels mature (Milner and Campbell, 2002). Thus, $\alpha_5\beta_1$ seems to promote angiogenesis in multiple settings, but, as noted above, one cannot assume that it is proangiogenic in all tissues and pathologies. In this study, we have explored the role of $\alpha_5\beta_1$ in choroidal neovascularization, the most common cause of severe vision loss in elderly Americans (Klein et al., 1993).

Materials and Methods

Mouse Model of Choroidal Neovascularization. Mice were treated in accordance with the Association for Research in Vision and Ophthalmology guidelines for the use of animals in research. Choroidal neovascularization was induced by laser photocoagulation-induced rupture of Bruch's membrane as described previously (Tobe et al., 1998). In brief, 5- to 6-week-old female C57BL/6J mice were anesthetized with ketamine hydrochloride (100 mg/kg body weight), and pupils were dilated with 1% tropicamide. Three burns of 532 nm diode laser photocoagulation (75-μm spot size, 0.1-s duration, 120 mW) were delivered to each retina with the slit lamp delivery system of an OcuLight GL diode laser (Iridex, Mountain View, CA) using a handheld cover slip as a contact lens to view the retina. Burns were performed in the 9, 12, and 3 o'clock positions of the posterior pole of the retina. Production of a bubble at the time of laser, which indicates rupture of Bruch's membrane, is an important factor in obtaining choroidal neovascularization; therefore, only burns in which a bubble was produced were included in the study.

Immunohistochemistry and Histochemistry. Two weeks after rupture of Bruch's membrane, mice were euthanized and eyes were removed and fixed for 30 min in 0.1 M phosphate buffer, pH 7.6, containing 4% paraformaldehyde and 5% sucrose. After 30 min, corneas and lenses were removed and then fixation was continued for another hour. After washing overnight with 0.1 M phosphate buffer containing 20% sucrose, the eyecups were frozen in optimum cutting temperature embedding compound (Miles Diagnostics, Elkhart, IN). Ocular frozen sections (10 μm) were dried with cold air for 20 min, fixed in freshly prepared 4% paraformaldehyde in 0.05 M phosphate-buffered saline (PBS) at room temperature for 15 min, and rinsed with 0.05 M Tris-buffered saline (TBS) for 10 min. Endogenous peroxidases were inhibited by a 15-min incubation with 0.75% H_2O_2 in methanol. Sections were washed three times in 0.05 M TBS and nonspecific binding sites were blocked by incubating in 10% normal goat serum in 50 mM TBS for 30 min at room temperature. Sections were incubated with 1:200 rabbit polyclonal antibody directed against α_5 integrin subunit (Chemicon, Temecula, CA) in 1% bovine serum albumin (BSA) in TBS at 4°C overnight. For controls, nonimmune IgG (Vector Laboratories, Burlingame, CA) was substituted for primary antibody. After two rinses with TBS, sections were incubated for 30 min at room temperature with secondary antibody,

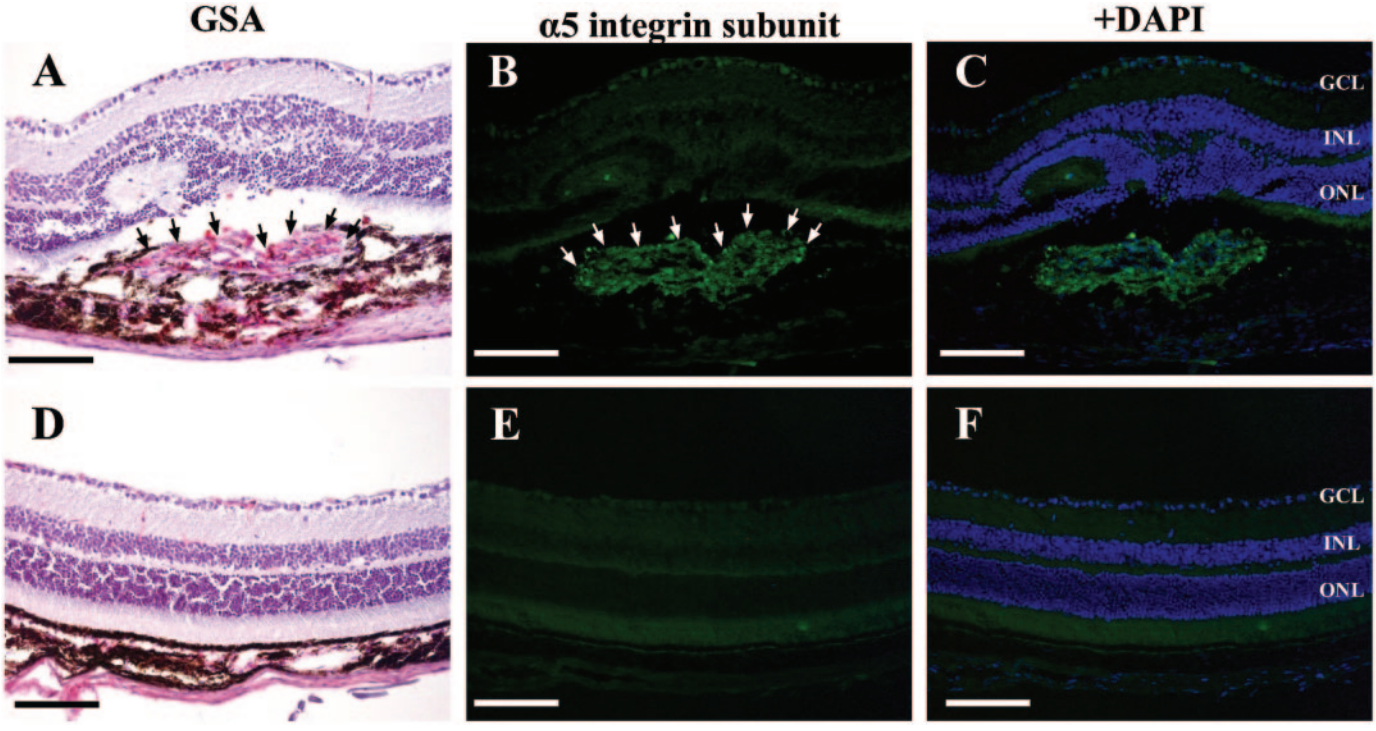

Fig. 1. Immunohistochemical staining for integrin α_5 subunit in mice with choroidal neovascularization. Adult C57BL/6J mice had laser-induced rupture of Bruch's membrane in each eye. Two weeks after laser treatment, mice were euthanized, eyes were removed, and frozen sections were cut through rupture sites. Some sections were stained with *Griffonia simplicifolia*, which selectively stains vascular cells and allows visualization of choroidal neovascularization (A). Adjacent sections were immunohistochemically stained for integrin α_5 subunit (B). Superimposed image from a DAPI-stained section shows the retinal cells in the ONL, inner nuclear layer (INL), and ganglion cell layer (GCL), confirming that the cells expressing α_5 integrin are in the subretinal space (C). Retina and choroid remote from Bruch's membrane rupture sites showed staining of retinal vessels with GSA, but no choroidal neovascularization (D) and no staining for integrin α_5 subunit (E and F). Scale bar, 100 μm.

1:1000 fluorescein isothiocyanate-conjugated goat anti-rabbit IgG F(ab′)2 (Jackson ImmunoResearch Laboratories Inc., West Grove, PA). Sections were counterstained with DAPI (Kirkegaard and Perry Laboratories, Gaithersburg, MD) and mounted with Aquamount (British Drug House, Poole, Dorset, UK).

Serial sections were stained with biotinylated *Griffonia simplicifolia* lectin B4 (GSA; Vector Laboratories) to identify choroidal neovascularization as described previously (Ozaki et al., 1998). In brief, slides were incubated in methanol/H_2O_2 for 10 min at 4°C, washed with 0.05 M TBS, pH 7.6, and incubated for 30 min in 10% normal porcine serum. Slides were incubated for 2 h at room temperature with biotinylated GSA. After washing, the slides were incubated in streptavidin-phosphatase and developed with HistoMark Red (Kirkegaard and Perry Laboratories) according to the manufacturer's instructions. Sections were dehydrated and mounted with Cytoseal. Stained sections were examined with a Nikon microscope and captured as digital files with a Nikon digital still camera (DXM1200; Nikon Instruments Inc., New York, NY).

Systemic Administration of JSM6427 in Mice with Rupture of Bruch's Membrane. Two different concentrations of JSM6427, 3 mg/ml in PBS and 20 mg/ml in 100 mM glycine/NaOH, pH 4.0, or the corresponding vehicle alone were loaded into osmotic mini-pumps (model 2002; Alza Corp., Palo Alto, CA) with internal volume of 200 μl and mean pumping rate of 0.5 μl/h. Pumps were implanted beneath the skin of the back and the following day the mice had laser-induced rupture of Bruch's membrane at 3 locations in each eye. After 14 days, the mice were perfused with 1 ml of PBS containing 50 mg/ml fluorescein-labeled dextran (2×10^6 average molecular

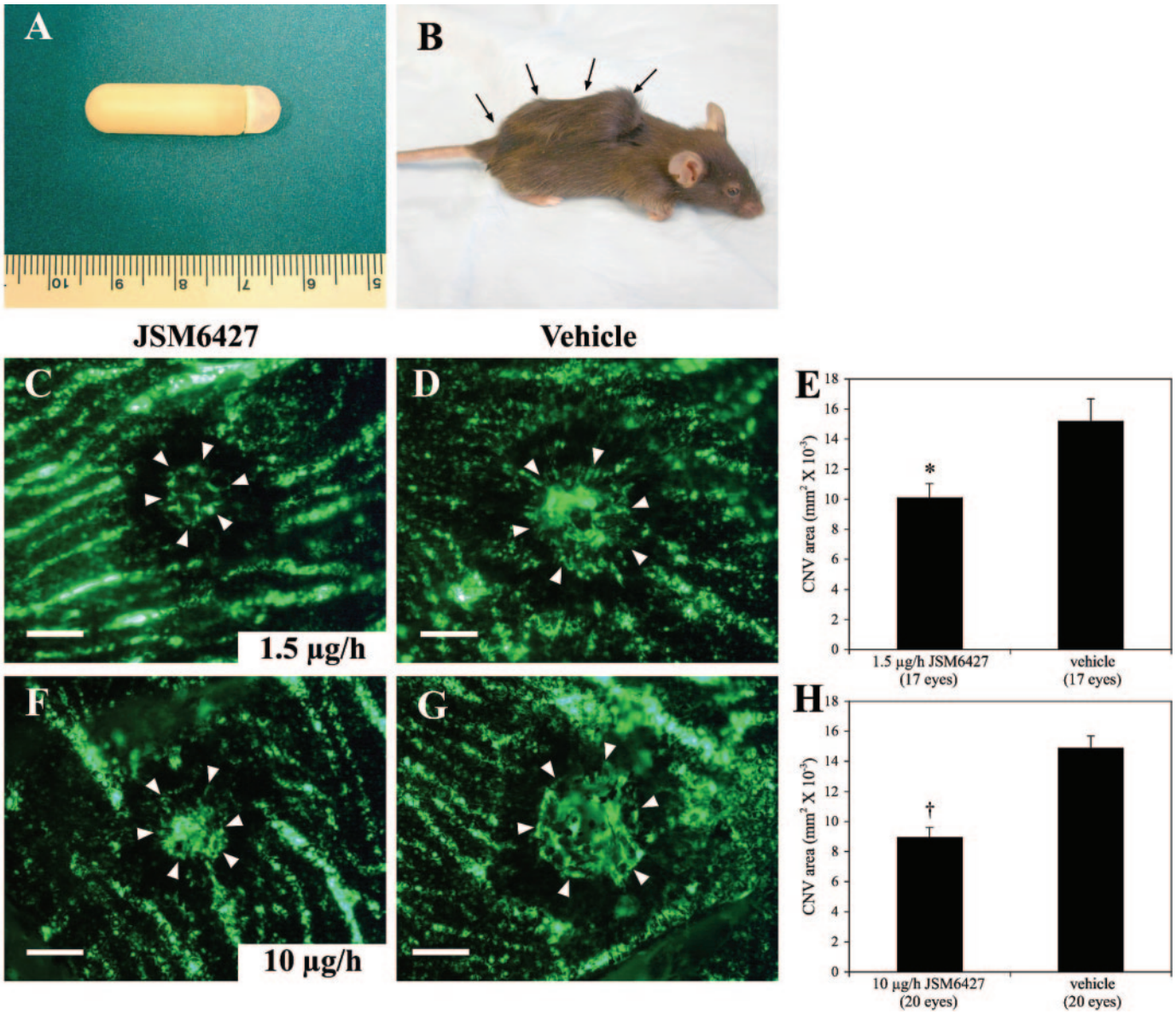

Fig. 2. Systemic delivery of JSM6427 by osmotic minipump suppresses the development of choroidal neovascularization at Bruch's membrane rupture sites. A, the osmotic minipumps were approximately 30 mm long. B, the implanted minipumps were visible as humps (arrows) beneath the skin of the back. Mice implanted with pumps containing 3 mg/ml JSM6427 received approximately 1.5 μg/h JSM6427 and choroidal flat mounts after perfusion with fluorescein-labeled dextran showed small areas of choroidal neovascularization at rupture sites (C, arrows) compared with areas of choroidal neovascularization seen in mice implanted with pumps containing vehicle (D, arrows). Image analysis confirmed that there was significantly less choroidal neovascularization in mice that received 1.5 μg/h JSM6427 compared with those that received vehicle (E). Mice implanted with pumps containing 20 mg/ml JSM6427 received approximately 10 μg/h JSM6427 and also seemed to have smaller areas of choroidal neovascularization (F, arrows) than mice that received vehicle (G, arrows). Image analysis showed a statistically significant difference from vehicle (H) in the same range as that seen after infusion of 1.5 μg/h of JSM6427.*, $p = 0.0005$; †, $p = 6 \times 10^{-8}$ by Mann-Whitney U test. Scale bar, 100 μm.

weight; Sigma-Aldrich, St. Louis, MO) and choroidal flat mounts were prepared as described previously. In brief, eyes were removed and fixed for 1 h in 10% phosphate-buffered formalin. The cornea, lens, and retina were removed, and four radial cuts were made in the eyecup, allowing it to be flat-mounted in aqueous mounting medium. Flat mounts were examined by fluorescence microscopy, and images were digitized using a three-color charge-coupled device video camera and a frame grabber. Image analysis software (Image-Pro Plus; Media Cybernetics, Silver Spring, MD) was used to measure the total area of choroidal neovascularization at each rupture site.

To assess the effect of JSM6427 on established choroidal neovascularization, mice had rupture of Bruch's membrane at three locations in each eye. After 7 days, 9 mice were perfused with fluorescein-labeled dextran, and the baseline area of neovascularization at each rupture site was measured. The remaining mice had implantation of osmotic minipumps containing 20 mg/ml JSM6427 in 100 mM sodium phosphate buffer, 50 mM NaCl, pH 7.4, or vehicle alone. At 7 days after implantation, some mice were euthanized for terminal terminal deoxynucleotidyl transferase dUTP nick-end labeling (TUNEL). The rest of the mice were perfused with fluorescein-labeled dextran 7 days after implantation, and the area of choroidal neovascularization at rupture sites was measured.

Intravitreous Injections of JSM6427. Mice had rupture of Bruch's membrane at three locations in each eye and were given an intravitreous injection of 1 μl of vehicle (PBS or 100 mM phosphate buffer, and 50 mM NaCl, pH 7.4) containing of 3 or 20 μg of JSM6427 in one eye and 1 μl of vehicle alone in the other eye on days 0 and 7. For an additional control, some mice received no injection. On day 14, the mice were perfused with fluorescein-labeled dextran, and the area of choroidal neovascularization at Bruch's membrane rupture sites was measured.

Identification of Apoptotic Cells in Vivo by TUNEL. Eyes were fixed in 4% paraformaldehyde in 0.1 M phosphate buffer and frozen in OCT. Serial 10-μm sections were cut through each rupture

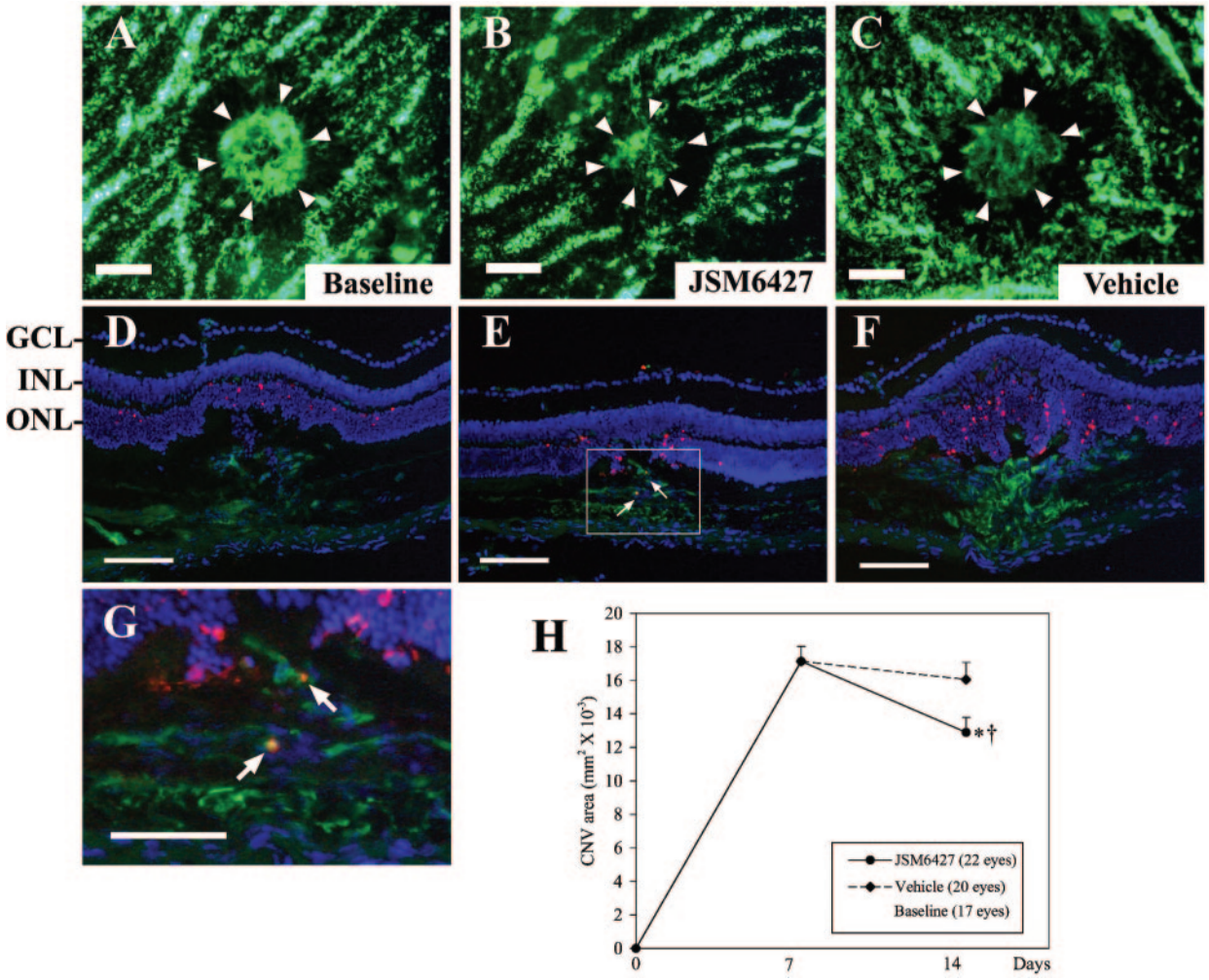

Fig. 3. Systemic delivery of JSM6427 by osmotic minipump causes regression of choroidal neovascularization. Adult C57BL/6J mice had laser-induced rupture of Bruch's membrane at three locations in each eye. Seven days after laser treatment, nine mice were perfused with fluorescein-labeled dextran, and the baseline amount of choroidal neovascularization at 7 days (A, arrows) was measured by image analysis. The remainder of the mice had implantation of an osmotic minipump containing 20 mg/ml JSM6427 (B) or vehicle (C), and these mice were perfused with fluorescein-labeled dextran on day 14. In mice that received JSM6427, the area of choroidal neovascularization lesions (B, arrows) appeared smaller than those in mice treated with vehicle (C, arrows) and the baseline amount seen at day 7 (A, arrows). TUNEL (red) of sections also stained with GSA, which stains vascular cells (green), and DAPI, which stains cell nuclei (blue), showed apoptotic cells in the ONL in day 7 baseline eyes (D), a consequence of the laser treatment 7 days before. Sections from day 14 eyes that had been treated with JSM6427 also showed apoptotic cells in the ONL, but in addition there were yellow cells within choroidal neovascularization lesions (E and G, arrows) as a result of colocalization of TUNEL and GSA, indicating apoptosis of cells with the choroidal neovascularization. Sections from eye treated with vehicle showed apoptotic cells in the ONL, but not within the choroidal neovascularization (F). Measurement of the area of choroidal neovascularization by image analysis confirmed that there was a significant reduction in mice treated with JSM6427 compared with the amount seen at baseline or in mice treated with vehicle (H). $*$, $p = 0.0039$ by linear mixed model for comparison with baseline; †, $p = 0.0283$ by linear mixed model for comparison with vehicle. P values were adjusted for multiple comparisons using Dunnett's method. Scale bars: A–F, 100 μm; G, 50 μm.

site. Sections were fixed with 1% paraformaldehyde for 10 min at room temperature, and TUNEL was done with the ApopTag Red kit (Chemicon International, Temecula, CA) according to the manufacturer's instructions. The sections were also histochemically stained with GSA as described above. Slides were also stained with DAPI and mounted in aqueous mounting medium.

Statistical Analysis. Data were analyzed using a linear mixed model accounting for possible correlations in measurements from the same mice. Dunnett's adjustment was made for multiple comparisons.

Solid Phase Binding Assay. The inhibiting activity and integrin selectivity of the integrin inhibitor was determined in a solid phase binding assay using soluble integrins and coated extracellular matrix protein. Binding of integrins was then detected by specific antibodies in an enzyme-linked immunosorbent assay. Fibronectin and vitronectin were purchased from Sigma (St Louis, MO). The integrin $\alpha_5\beta_1$ extracellular domain Fc-fusion protein was a generous gift from M. Humphries (University of Manchester), and $\alpha_V\beta_3$ was purchased from Chemicon (Chemicon Europe, Germany). The integrin antibodies were purchased from Pharmingen, BD Bioscience Europe ($\alpha_V\beta_3$), and Sigma (anti-human-Fc-HRP antibody conjugate and anti-mouse-HRP conjugate).

The detection of HRP was performed using HRP substrate solution 3.3.5.5′-tetramethylethylenediamine (Seramun Diagnostica GmbH, Dolgenbrodt, Germany) and 1 M H_2SO_4 for stopping the reaction. The developed color was measured at 450 nm.

$\alpha_5\beta_1$:Nunc-Immuno maxisorp plates (Nalge Nunc International, Rochester, NY) were coated over night at 4°C with fibronectin (0.25 μg/ml) in 15 mM Na_2CO_3, 35 mM $NaHCO_3$, pH 9.6. All subsequent washing and binding were performed in 25 mM Tris, pH 7.6, 150 mM NaCl, 1 mM $MnCl_2$, and 1 mg/ml BSA. The plates were blocked with 3% BSA in PBS 0.1% Tween 20 for 1 h at room temperature. Soluble integrin $\alpha_5\beta_1$ (0.5 μg/ml) and a serial dilution of integrin inhibitor were incubated in the coated wells for 1 h at room temperature. The detection antibody (anti-human-Fc-HRP antibody conjugate) was then applied for 1 h at room temperature, and the binding was visualized as described above. For the $\alpha_V\beta_3$ assay, plates were coated with vitronectin (1 μg/ml) and blocked as described for $\alpha_5\beta_1$. Soluble $\alpha_V\beta_3$ (1 μg/ml) was incubated with a serial dilution of integrin inhibitor for 1 h at room temperature. Primary (anti-$\alpha_V\beta_3$) and secondary antibody (anti-mouse-HRP conjugate) were applied for 1 h at RT, and the binding was visualized as described above. All IC_{50} measurements were performed at least 30 times.

Identification of Apoptotic Cells in Vitro by TUNEL and Fluorescent Activated Cell Sorting. Human umbilical vein endothelial cells were maintained in endothelial cell growth medium (PromoCell, Heidelberg, Germany) and grown to 80% confluence, trypsinized, and preincubated for 20 min in serum-free medium alone or medium containing 100 nM, 500 nM, 1 μM, 10 μM, 25 μM, or 50 μM JSM6427 or 10 μM camptothecin. Cells (4×10^5) were plated in six-well plates coated with 10 μg/ml fibronectin (Chemicon Europe, Hampshire, UK) and grown for 48 h. Adherent and nonadherent cells were collected, pooled, and washed. Cells were fixed in 1% paraformaldehyde for 30 min on ice, washed, and carefully resuspended in 70% ice-cold ethanol. TUNEL was performed using the APO-Direct kit (BD Pharmingen, San Diego, CA). In brief, cells were incubated with TdT enzyme and fluorescein isothiocyanate-dUTP in reaction buffer for 60 min (positive and negative cells of the kit) or 180 min (probes) at 37°C. Cells were rinsed and incubated with PI-staining solution for 30 min to determine total cell numbers. Fluorescence-activated cell sorting analysis was performed using a FACSCalibur (BD Bioscience, San Diego, CA) and the CellQuest software.

Western Blotting. ARPE19 cells were incubated in serum-free Dulbecco's modified Eagle's medium/Ham's F12 (Biochrom AG, Berlin, Germany) culture medium for 16 h. Plates were coated with 10 μg/ml fibronectin or 0.002% poly-L-lysine (Sigma-Aldrich, Munich, Germany) and blocked with 1% BSA. Cells were trypsinized and held in suspension for 30 min. Subsequently, 1×10^6 cells were incubated with compounds for 10 min. Cells were allowed to adhere for 15 min on fibronectin in serum-free medium. Adherent cells and cells from supernatants were lysed in 150 μl of lysis buffer (1% Nonidet P-40, 150 mM NaCl, 50 mM Tris-HCl, pH 7.5, protease inhibitor cocktail (Sigma-Aldrich), 25 mM glycerophosphate, 50 mM NaF, 10 mM $Na_4P_2O_7$, and 1 mM orthovanadate) on ice. Lysates were centrifuged, and equal amounts of protein were separated on a 4 to 15% Tris/HCl gel by SDS-polyacrylamide gel electrophoresis and transferred to polyvinylidene difluoride membranes by semi-dry Western blotting. Membranes were blocked in 3% BSA. Phosphorylated extracellular signal regulated kinase (ERK) and total ERK were detected with a phospho-specific ERK1/2 (pThr202/pTyr204) antibody (Cell Signaling, Danvers, MA) and a p44/42 mitogen-activated protein kinase kinase antibody (Cell Signaling). Bands were visualized with peroxidase-conjugated anti-rabbit and anti-mouse antibodies (Sigma-Aldrich) and BM chemiluminescence Western blotting peroxidase substrate (Roche Applied Science, Mannheim, Germany). The luminescence signal was measured and quantified using a Lumi imager (Roche) and corresponding software.

Results

Expression of Integrin α_5 Subunit Is Increased in Vascular Cells Participating in Choroidal Neovascularization. Two weeks after laser-induced rupture of Bruch's membrane staining with GSA showed large choroidal neovascularization lesions at rupture sites (Fig. 1A, arrows). Adjacent sections immunohistochemically stained for integrin α_5 subunit showed strong labeling throughout the entire choroidal neovascularization lesion (Fig. 1B, arrows). Superimposed images from DAPI-stained sections showed the overlying neural retina, confirming that the cells labeled with anti-α_5 are in the subretinal space (Fig. 1C). Regions of retina remote from Bruch's membrane rupture sites showed no choroidal neovascularization and no staining for α_5 subunit (Fig. 1, D–F). This suggests that expression of α_5 subunit in vascular cells in the eye under normal circumstances is below the sensitivity of our staining technique to detect it, but there is strong up-regulation of α_5 subunit expression in vascular cells participating in choroidal neovascularization.

JSM6427 Is a Selective Antagonist of Integrin $\alpha_5\beta_1$. The integrin inhibitor JSM6427 is an antagonist of binding to integrin $\alpha_5\beta_1$ and is at least 1200-fold less potent in the inhibition of binding to $\alpha_V\beta_3$, the integrin that is most closely

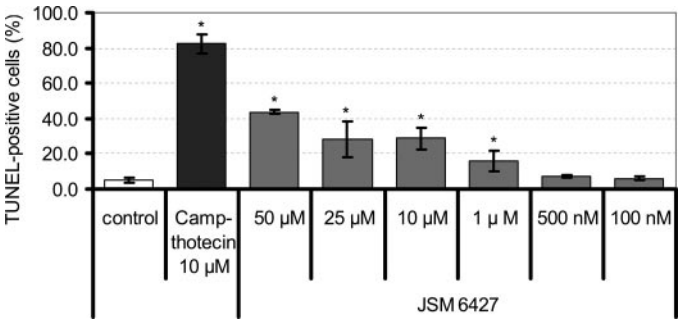

Fig. 4. JSM6427 induces apoptosis in cultured vascular endothelial cells. Human umbilical vein endothelial cells were grown in fibronectin coated dishes for 48 h in serum-free medium containing various concentrations of JSM6427 or camptothecin. TUNEL-stained cells were detected by fluorescence-activated cell sorting. Each bar shows the mean (± S.D.) percentage of apoptotic cells per culture generated from one experiment performed in triplicate. *, $p < 0.01$ by ANOVA with Dunnett's correction for multiple comparisons.

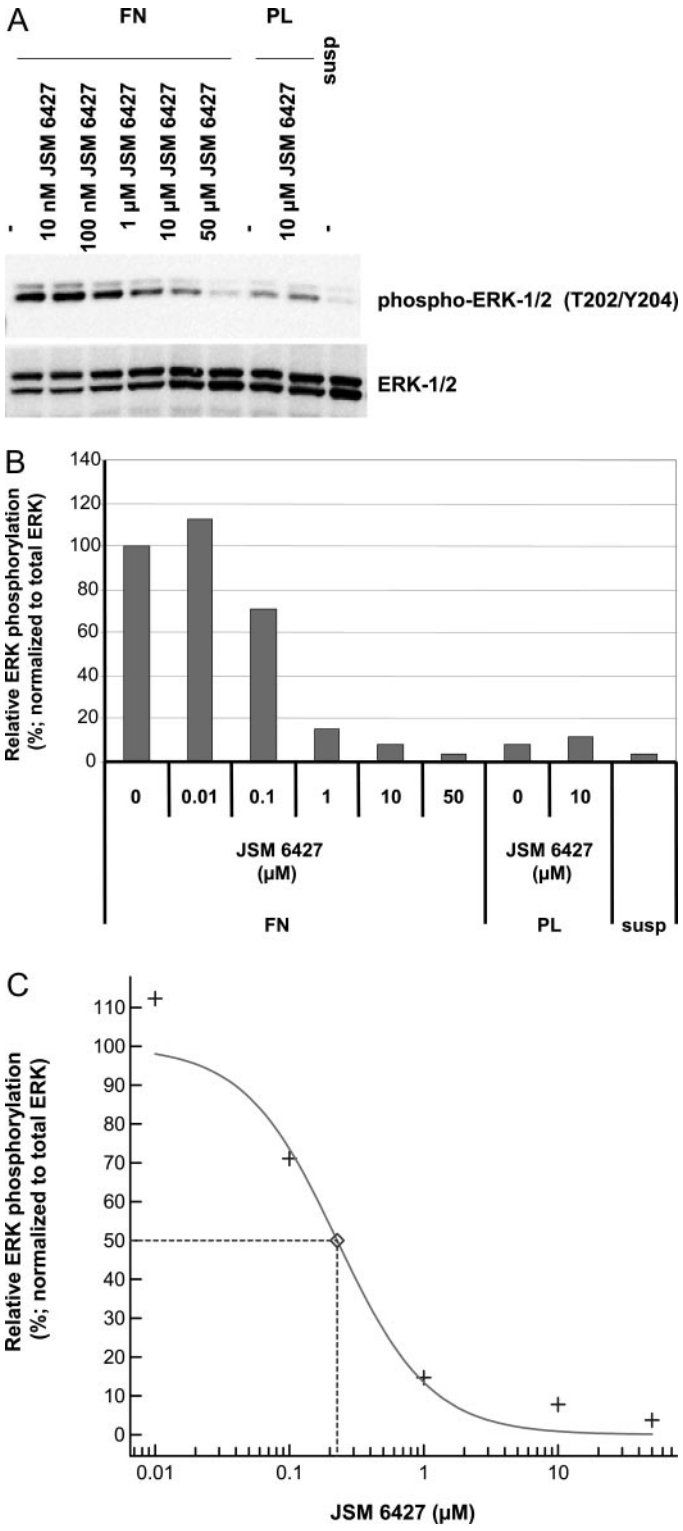

Fig. 5. JSM6427 reduces fibronectin-induced phosphorylation of ERK. Serum starved ARPE19 cells were preincubated in suspension for 10 min with serum-free medium or medium containing various concentrations of JSM6427. The cells were then kept in suspension (susp) or plated on fibronectin (FN) or poly-L-lysine (PL). After 15 min, cells were lysed and the lysates were run in Western blots using an antibody directed against phosphorylated ERK or ERK. A, Western blots showed that for cells not preincubated in JSM6427, those plated on FN had a much stronger signal for phosphorylated ERK than those plated on poly-L-lysine or those kept in suspension. Preincubation with JSM6427 before plating on FN caused a dose-dependent reduction in the amount of phosphorylated ERK in the cultures. B, band intensity on Western blots was quantified using a Lumi Imager. The amount of phosphorylated ERK was normalized to the total amount of ERK and the phosphorylation of cells plated on fibronectin was set at 100%. This quantification confirmed that JSM6427 reduced fibronectin-induced phosphorylation of ERK. Preincubation with 10 μM JSM6427 completely eliminated the fibronectin-induced stimulation of ERK phosphorylation. C, the IC_{50} value was calculated using XLFit software. All of these results were replicated in an independent experiment.

related to $\alpha_5\beta_1$ in structure. The selectivity against other integrins such as $\alpha_V\beta_5$ and $\alpha_{IIb}\beta_3$ is significantly higher, 3700-fold or >100,000-fold, respectively (data not shown).

Subcutaneous Delivery of JSM6427 Suppresses Choroidal Neovascularization. Osmotic minipumps (Fig. 2A) that release 1.5 or 10 μg/h JSM6427 or vehicle alone were implanted beneath the skin on the backs of mice (Fig. 2B), and the following day, Bruch's membrane was ruptured in three locations in each eye. Fourteen days after rupture of Bruch's membrane, the size of choroidal neovascularization lesions at rupture sites in mice that received 1.5 or 10 μg/h JSM6427 (Fig. 2, C and F) appeared smaller than corresponding control mice that received infusion of vehicle (Fig. 2, D and G). Measurement of the size of the lesions by image analysis confirmed that for both infusion rates of JSM6427, 1.5 (Fig. 2E) and 10 μg/h (Fig. 2H), choroidal neovascularization lesions were significantly smaller than those in corresponding vehicle-treated control mice by approximately 33 and 40%, respectively.

Subcutaneous Delivery of JSM6427 Causes Regression of Established Choroidal Neovascularization. Mice had laser-induced rupture of Bruch's membrane, and after 7 days, some mice were used to measure the baseline amount of choroidal neovascularization (Fig. 3A). In the remainder of the mice, an osmotic minipump was implanted that released 10 μg/h JSM6427 or vehicle. After 7 days of treatment, the mice infused with JSM6427 had small choroidal neovascularization lesions at Bruch's membrane rupture sites (Fig. 3B), whereas mice infused with vehicle had lesions that appeared larger (Fig. 3C). TUNEL showed labeling within the outer nuclear layer (ONL) of the retina overlying choroidal neovascularization in day 7 baseline eyes (Fig. 3D). This was probably a consequence of the laser photocoagulation that was used to induce rupture of Bruch's membrane, although it is possible that the presence of choroidal neovascularization is damaging to the overlying retina as a result of interference with transmission of oxygen from the choroid, interference with transmission of survival signals from the retinal pigmented epithelium, or some other reason. At 14 days after rupture of Bruch's membrane, mice infused with JSM6427 for the previous 7 days (Fig. 3E) and those infused with vehicle (Fig. 3F) showed apoptosis in the retina overlying choroidal neovascularization, but only the mice infused with JSM6427 showed apoptosis of vascular cells within the choroidal neovascularization as expected for the proposed mechanism of action and confirmed with in vitro apoptosis assays (Fig. 4). Figure 3G shows the boxed region in Fig. 3E at high magnification, providing better visualization of two yellow cells (arrows) because of colocalization of GSA and ApopTag red. Measurement of the size of choroidal neovascularization lesions by image analysis showed that mice infused with JSM6427 had significantly smaller lesions than those seen at baseline or those seen in mice infused with vehicle (Fig. 3H). This indicates that continuous systemic

infusion of JSM6427 causes regression of choroidal neovascularization.

JSM6427 Causes Apoptosis of Vascular Endothelial Cells in Vitro. Human umbilical vein endothelial cells were grown in fibronectin-coated wells for 48 h in serum-free medium containing various concentrations of JSM6427. Camptothecin, a strong inducer of apoptosis, was used as a positive control. JSM6427 caused a dose-dependent increase in the percentage of TUNEL-positive cells in cultures ranging from 44% for those incubated with 50 μM to 6% for those incubated in 100 nM (Fig. 4). In cultures incubated in serum-free medium, 5% of cells were TUNEL-positive and 82% of cells were labeled in cultures incubated with 10 μM camptothecin. These data show that JSM6427 induces apoptosis of vascular endothelial cells.

JSM6427 Reduces Fibronectin-Induced Phosphorylation of ERK. The mechanism by which ECM components generate survival signals through integrins involves increased phosphorylation of intracellular messengers that increase expression of apoptosis inhibitors such as Bcl-2 (Lee and Ruoslahti, 2005). Phosphorylation of ERK plays a central role in fibronectin-mediated survival signaling through $\alpha_5\beta_1$ in brain capillary endothelial cells (Wang and Milner, 2006). Therefore, we investigated the effect of JSM6427 on fibronectin-induced phosphorylation of ERK in ARPE19 cells, which express $\alpha_5\beta_1$. Serum-starved ARPE19 cells were preincubated with JSM6427 for 10 min in suspension and plated for 15 min on fibronectin, poly-L-lysine, or kept in suspension. Western blots showed that for cells not preincubated in JSM6427, those plated on fibronectin had a much stronger signal for phosphorylated ERK than those plated on poly-L-lysine or those kept in suspension (Fig. 5A). Preincubation with JSM6427 before plating on fibronectin caused a dose-dependent reduction in the amount of phosphorylated ERK in the cultures. Quantification of the signal for phosphorylated ERK normalized to the total amount of ERK showed that preincubation with 10 μM JSM6427 completely eliminated the fibronectin-induced stimulation of ERK phosphorylation (Fig. 5B), and the IC_{50} was 0.23 μM (Fig. 5C).

Two Intravitreous Injections of JSM6427 Did Not Cause Significant Suppression of Choroidal Neovascularization. To explore the feasibility of local delivery of JSM6427, mice had laser-induced rupture of Bruch's membrane followed by intravitreous injection of vehicle or vehicle containing 3 or 20 μg of JSM6427 immediately after laser treatment and 7 days later. Fourteen days after laser treatment, the area of choroidal neovascularization was measured by image analysis. The size of choroidal neovascularization lesions appeared somewhat smaller in eyes treated with JSM6427, but there was not a statistically significant difference compared with vehicle-treated or untreated eyes (Fig. 6). This suggests that weekly intravitreous injections in mice are not able to maintain levels of JSM6427 sufficient to significantly inhibit choroidal neovascularization.

Discussion

In this study, we have shown that $\alpha_5\beta_1$ integrin is strongly up-regulated in choroidal neovascularization. This marked differential in expression between vascular cells participating in choroidal neovascularization and vascular cells in established choroidal vessels, suggests that $\alpha_5\beta_1$ may play an important role in growth and maintenance of the new vessels, and blocking $\alpha_5\beta_1$ may provide a way to selectively target choroidal neovascularization. Using a selective antagonist of $\alpha_5\beta_1$, JSM6427, we found this to be the case. Sustained systemic delivery of JSM6427 using an osmotic minipump suppressed the de-

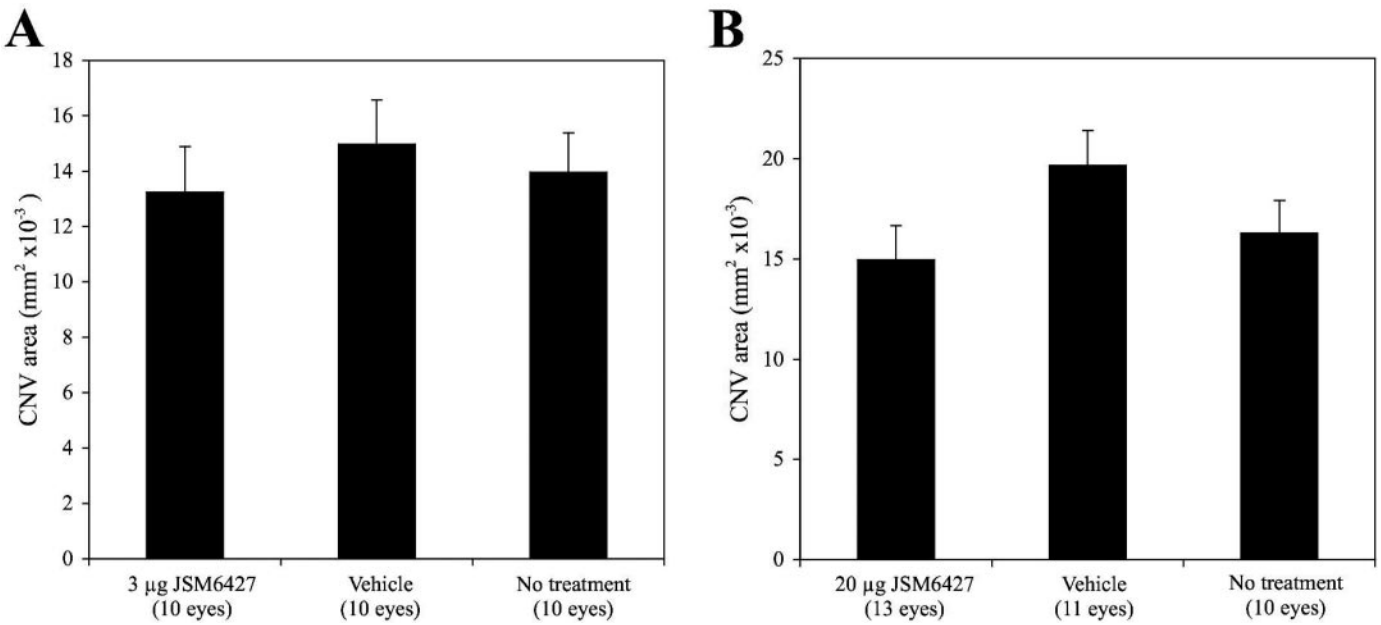

Fig. 6. Two intravitreous injections of JSM6427 failed to suppress choroidal neovascularization at Bruch's membrane rupture sites. Adult C57BL/6J mice had rupture of Bruch's membrane at three locations in each eye. On days 0 and 7 after laser treatment, mice were given an intravitreous injection of 3 or 20 μg of JSM6427 in one eye and vehicle in the fellow eye. At day 14, mice were perfused with fluorescein-labeled dextran and the area of choroidal neovascularization at Bruch's membrane rupture sites was measured by image analysis. There was no statistically significant difference in the size of choroidal neovascularization lesions in eyes injected with 3 (A) or 20 μg (B) of JSM6427 compared with either fellow eyes treated with vehicle or uninjected eyes.

velopment of choroidal neovascularization, and when infusion was started after the neovascularization was established, it caused it to regress. TUNEL staining showed selective apoptosis in vascular cells participating in the neovascularization in JSM6427-treated mice. This suggests that signaling through $\alpha_5\beta_1$ provides a critical survival signal to endothelial cells in choroidal new vessels that, when blocked, triggers apoptosis. Endothelial cells in established vessels must develop alternative survival signal pathways that eliminate the dependence on $\alpha_5\beta_1$ signaling manifested by endothelial cells in choroidal neovascular lesions. Such a switch has been noted when cerebral vessels mature and change from an angiogenic to a mature phenotype; they stop expressing $\alpha_5\beta_1$ and $\alpha_4\beta_1$, and begin to express $\alpha_1\beta_1$ and $\alpha_6\beta_1$ (Milner and Campbell, 2002). The exquisite selectivity for JSM6427-induced apoptosis for endothelial cells in choroidal neovascularization compared with mature choroidal vessels predicts a good safety profile.

Cell signaling through which integrins promote cells survival is complex (for review, see Giancotti and Ruoslahti, 1999). Binding of most integrins to a ligand in the ECM activates focal adhesion kinase, which plays a role in most integrin-mediated effects; survival signaling occurs by activation of focal adhesion kinase along with other signaling molecules that act together to increase levels of Bcl-2 or other inhibitors of apoptosis (Lee and Ruoslahti, 2005). Phosphorylation of ERK plays a central role in stimulation of brain capillary endothelial cell survival by fibronectin through $\alpha_5\beta_1$ (Wang and Milner, 2006). JSM6427 blocks fibronectin-induced phosphorylation of ERK, which probably plays a role in its induction of apoptosis.

Despite the apparent safety of sustained systemic administration of JSM6427, local administration has the theoretical benefit of limiting exposure to the rest of the body and reducing the total amount of JSM6427 that is required for treatment. Two intravitreous injections of JSM6427 over the course of 2 weeks failed to suppress choroidal neovascularization. A possible explanation is that sustained exposure of JSM6427 to endothelial cells in choroidal neovascular lesions is necessary to perturb survival signals, and even brief lapses in blockade of $\alpha_5\beta_1$ signaling may be sufficient to prevent apoptosis. In the future, it will be worthwhile to test this hypothesis by assessing the effect of sustained local delivery of JSM6427.

Choroidal neovascularization occurs in diseases of the retinal pigmented epithelium/Bruch's membrane complex. The most common of these is age-related macular degeneration, which is the most prevalent cause of severe vision loss in patients over the age of 60 in developed countries (Klein et al., 1993). Studies in animal models have demonstrated that VEGF is an important stimulus and that VEGF antagonists suppress the neovascularization (Kwak et al., 2000; Kryzstolik et al., 2002; Saishin et al., 2003). The role of VEGF in patients with neovascular age-related macular degeneration has now been confirmed in a clinical trial demonstrating that multiple intravitreous injections of pegaptanib, an aptamer that binds VEGF, slows the rate of visual loss (Gragoudas et al., 2004). This is a useful start to pharmacotherapy for choroidal neovascularization, but further improvements are needed. Regression of choroidal neovascularization is not achieved in patients treated with pegaptanib; the size of lesions continued to increase over the course of a year, although at a slower rate than that seen in patients that did not receive pegaptanib. Antagonism of VEGF seems to reduce excessive permeability and slows growth, but does not cause involution of choroidal neovascularization. VEGF provides some survival signals to newly developed endothelial cells (Alon et al., 1995), but survival signals from the extracellular matrix may be sufficient to allow continued growth of choroidal neovascular lesions, although at a slower rate. Combination treatment using JSM6427 with a VEGF antagonist may be extremely useful because perturbation of at least one source of matrix-derived survival signaling along with elimination of the survival signal provided by VEGF may be an effective means to promote involution of choroidal neovascularization.

Acknowledgments

We thank Sascha Birkner for assistance with some of the in vitro experiments.

References

Alon T, Hemo I, Itin A, Pe'er J, Stone J, and Keshet E (1995) Vascular endothelial growth factor acts as a survival factor for newly formed retinal vessels and has implications for retinopathy of prematurity. *Nat Med* **1:**1024–1028.

Bardos JI, Chau NM, and Ashcroft M (2004) Growth factor mediated induction of HDM2 positively regulates hypoxia-inducible factor 1alpha expression. *Mol Cell Biol* **24:**2905–2914.

Brooks P, Clark R, and Cheresh D (1994a) Requirement of vascular integrin alpha-v beta-3 for angiogenesis. *Science (Wash DC)* **264:**569–571.

Brooks PC, Montgomery AM, Rosenfeld M, Reisfeld RA, Hu T, Klier G, and Cheresh D (1994b) Integrin alpha v beta 3 antagonists promote tumor regression by inducing apoptosis of angiogenic blood vessels. *Cell* **79:**1157–1164.

Collo G and Pepper MS (1999) Endothelial cell integrin alpha5beta1 expression is modulated by cytokines and during migration *in vitro*. *J Cell Sci* **112:**569–578.

Giancotti FG and Ruoslahti E (1999) Integrin signaling. *Science (Wash DC)* **285:**1028–1032.

Gragoudas ES, Adamis AP, Cunningham ET Jr, Feinsod M, and Guyer DR (2004) Pegaptanib for neovascular age-related macular degeneration. *N Engl J Med* **351:**2805–2816.

Haddad JJ and Harb HL (2005) Cytokines and the regulation of hypoxia-inducible factor (HIF)-1alpha. *Int Immunopharmacol* **5:**461–483.

Hammes H, Brownlee M, Jonczyk A, Sutter A, and Preissner K (1996) Subcutaneous injection of a cyclic peptide antagonist of vitronectin receptor-type integrins inhibits retinal neovascularization. *Nat Med* **2:**529–533.

Hynes RO (2002) A reevaluation of integrins as regulators of angiogenesis. *Nat Med* **8:**918–921.

Kim S, Bell K, Mousa SA, and Varner JA (2000) Regulation of angiogenesis in vivo by ligation of integrin alpha5beta1 with the central cell-binding domain of fibronectin. *Am J Pathol* **156:**1345–1362.

Klein R, Klein BEK, and Linton KP (1993) The Beaver Dam Eye Study: the relation of age-related maculopathy to smoking. *Am J Epidemiol* **137:**190–200.

Kryzstolik MG, Afshari MA, Adamis AP, Gaudreault J, Gragoudas ES, Michaud NM, Li W, Connolly E, O'Neill CA, and Miller JW (2002) Prevention of experimental choroidal neovascularization with intravitreal anti-vascular endothelial growth factor antibody fragment. *Arch Ophthalmol* **120:**338–346.

Kwak N, Okamoto N, Wood JM, and Campochiaro PA (2000) VEGF is an important stimulator in a model of choroidal neovascularization. *Investig Ophthalmol Vis Sci* **41:**3158–3164.

Lee B-H and Ruoslahti E (2005) Alpha5beta1 integrin stimulates Bcl-2 expression and cell survival through Akt, focal adhesion kinase and Ca^{2+}/calmodulin-dependent protein kinase IV. *J Cell Biochem* **95:**1214–1223.

Luna J, Tobe T, Mousa SA, Reilly TM, and Campochiaro PA (1996) Antagonists of integrin alpha-v beta-3 inhibit retinal neovascularization in a murine model. *Lab Investig* **75:**563–573.

Magnussen A, Kasman IM, Norberg S, Baluk P, Murray R, and McDonald DM (2005) Rapid access of antibodies to alpha5beta1 integrin overexpressed on the luminal surface of tumor blood vessels. *Cancer Res* **65:**2712–2721.

Manalo DJ, Rowan A, Lavoie T, Natarajan L, Kelly BD, Ye SQ, Garcia JG, and Semenza GL (2005) Transcriptional regulation of vascular endothelial cell responses to hypoxia by HIF-1. *Blood* **105:**659–669.

Milner R and Campbell IL (2002) Developmental regulation of beta1 integrins during angiogenesis in the central nervous system. *Mol Cell Neurosci* **20:**616–626.

Ozaki H, Okamoto N, Ortega S, Chang M, Ozaki K, Sadda S, Vinores MA, Derevjanik N, Zack DJ, Basilico C, et al. (1998) Basic fibroblast growth factor is neither necessary nor sufficient for the development of retinal neovascularization. *Am J Pathol* **153:**757–765.

Parsons-Wingerter P, Kasman IM, Norberg S, Magnussen A, Zanivan S, Rissone A, Baluk P, Favre CJ, Jeffry U, Murray R, et al. (2005) Uniform overexpression and rapid accessibility of alpha5beta1 integrin on blood vessels in tumors. *Am J Pathol* **167:**193–211.

Ribatti D (2005) The crucial role of vascular permeability factor/vascular endothelial growth factor in angiogenesis: a historical review. *Br J Haematol* **128:**303–309.

Saishin Y, Saishin Y, Takahashi K, Lima e Silva R, Hylton D, Rudge JS, Wiegand SJ, and Campochiaro PA (2003) VEGF-TRAP$_{R1R2}$ suppresses choroidal neovascularization and VEGF-induced breakdown of the blood-retinal barrier. *J Cell Physiol* **195:**241–248.

Sottile J (2004) Regulation of angiogenesis by extracellular matrix. *Biochim Biophys Acta* **1654:**13–22.

Stoeltzing O, Liu W, Reinmuth N, Fan F, Parry GC, Parikh AA, McCarty MF, Bucana CD, Mazar AP, and Ellis LM (2003) Inhibition of integrin alpha5beta1 function with a small peptide (ATN-161) plus continuous 5-FU infusion reduces colorectal liver metastases and improves survival in mice. *Int J Cancer* **104:**496–503.

Tobe T, Ortega S, Luna JD, Ozaki H, Okamoto N, Derevjanik NL, Vinores SA, Basilico C, and Campochiaro PA (1998) Targeted disruption of the *FGF2* gene does not prevent choroidal neovascularization in a murine model. *Am J Pathol* **153:** 1641–1646.

Wang J and Milner R (2006) Fibronectin promotes brain capillary endothelial cell survival and proliferation through alpha$_5$beta$_1$ and alpha$_v$beta$_3$ integrins via MAP kinase signalling. *J Neurochem* **96:**148–159.

Yang JT, Rayburn H, and Hynes RO (1993) Embryonic mesodermal defects in alpha5 integrin-deficient mice. *Development* **119:**229–238.

Address correspondence to: Dr. Peter A. Campochiaro, The Johns Hopkins University School of Medicine, 600 N. Wolfe Street, Baltimore, MD 21287-9277. E-mail: pcampo@jhmi.edu